Australian Government
Department of Defence
Defence Science and
Technology Organisation

A Technique for Measurement of Static and Dynamic Longitudinal Aerodynamic Derivatives Using the DSTO Water Tunnel

Daniel M. Newman [1]

[1] **Quantitative Aeronautics Pty Ltd**

Defence Science and Technology Organisation

DSTO–TR–2599

ABSTRACT

The DSTO water tunnel's balance and rotary support mechanism provides a measurement capability for longitudinal dynamic derivatives. This report documents the underlying theory and computational implementation of a technique which uses the water tunnel for determination of normal force and pitching moment coefficient derivatives with respect to angle of attack, non-dimensional pitch rate and angle of attack rate.

Published by

DSTO Defence Science and Technology Organisation
506 Lorimer St,
Fishermans Bend, Victoria 3207, Australia

Telephone: (03) 9626 7000
Facsimile: (03) 9626 7999

AR No. AR-015-087
December, 2011

APPROVED FOR PUBLIC RELEASE

A Technique for Measurement of Static and Dynamic Longitudinal Aerodynamic Derivatives Using the DSTO Water Tunnel

Executive Summary

Determination of an aircraft's dynamic derivatives is an essential prerequisite for accurate modelling of linearised stability and control characteristics. DSTO operates an Eidetics Model 1520 water tunnel, which has been used extensively for flow visualisation tasks involving complete aircraft models. The water tunnel model support mechanism has been modified to allow independent or combined programmed rotational motions in pitch, roll and yaw, and to measure time-varying aircraft loads during motion using either two-component or five-component sting-mounted balances. Because the model support mechanism is restricted to rotational motion, the individual longitudinal dynamic derivatives can not be measured directly. However, combinations of measurements allow all the individual derivatives to be determined. This report details the underlying theory, computational implementation and experimental techniques associated with the measurement of aircraft longitudinal static and dynamic aerodynamic derivatives in the water tunnel.

The individual components of the main longitudinal dynamic derivatives are resolved from measurements using purely rotary oscillations, by combining results measured with different balance sting lengths. Experiments with simulated inputs have confirmed the general validity of the technique, and provided some indication of the data quality from which acceptable results might be obtained.

The difference between tunnel test and flight Reynolds number is large enough to potentially affect the validity of measured dynamic derivatives, depending on the geometry of the aircraft under test. The discrepancy should be specifically considered when planning a dynamic derivative test program. Owing to the small scales, low dynamic pressures and consequent low loads involved in the water tunnel balance system, and the structure of the computational treatment of the experimental results, results of acceptable quality require rigorous control of accuracy and precision at every stage of the experimental and computational process. Measurement and quality control of balance and model geometry are particularly important.

Static and combined dynamic derivatives can be reliably and accurately computed in the presence of very high noise levels on the measured signals, but separated dynamic derivatives require signal-to-noise ratios in the order of 100 dB or better for adequate performance.

Author

Daniel M Newman
Quantitative Aeronautics Pty Ltd

Dan Newman wrote this report while under contract to DSTO. He holds BE, MEngSc and PhD degrees from the University of Sydney Department of Aeronautical Engineering, and is a performance and flying qualities flight test engineering graduate of the US Naval Test Pilot School. He served in the RAAF for eight years to 1985, spending much of that time at ARDU. From 1985 to 1996 he worked as a tutor and lecturer in the University of Sydney Department of Aeronautical Engineering, performing teaching and research in flight mechanics, aerodynamics and aeroelasticity. Since 1997 he has worked for various aerospace organisations, including serving as a civilian flight test engineer on several RAAF simulator data gathering programs and completing numerous software development, flight mechanics and aerodynamics tasks for DSTO.

Contents

Appendices

Glossary

AIAA	American Institute of Aeronautics and Astronautics
ARC	British Aeronautical Research Council
AVD	Air Vehicles Division
DATCOM	Data Compendium
DSTO	Defence Science and Technology Organisation
FSB	Flight Systems Branch
IAPWS	International Association for the Properties of Water and Steam
IEEE	Institute of Electrical and Electronics Engineers
ISO	International Organization for Standardization
NASA	US National Aeronautics and Space Administration
SDM	Standard Dynamics Model
SNR	Signal-to-noise ratio

Notation

$\mathbf{A}$	Angular position and velocity sample matrix	11
$\mathbf{A_R}$	Reduced angular position and velocity sample matrix (has several possible forms)	11
C_l	Rolling moment coefficient: $\frac{L}{\frac{1}{2}\rho V^2 S\bar{c}}$	4
C_m	Pitching moment coefficient: $\frac{M}{\frac{1}{2}\rho V^2 S\bar{c}}$	3
C_{m_o}	Pitching moment coefficient in steady reference condition	5
C_{m_q}	Pitching moment coefficient derivative with respect to non-dimensional pitch rate (pitch damping): $\frac{\partial C_m}{\partial q}\frac{2V}{\bar{c}}$	6
C_{m_α}	Pitching moment coefficient derivative with respect to angle of attack (pitch stiffness): $\frac{\partial C_m}{\partial \alpha}$	6
$C_{m_{\dot{\alpha}}}$	Pitching moment coefficient derivative with respect to non-dimensional angle of attack rate: $\frac{\partial C_m}{\partial \dot{\alpha}}\frac{2V}{\bar{c}}$	6
$\mathbf{C_m}$	Column vector of pitching moment coefficient samples	10
C_n	Yawing moment coefficient: $\frac{N}{\frac{1}{2}\rho V^2 S\bar{c}}$	4
C_X	X force coefficient: $\frac{X}{\frac{1}{2}\rho V^2 S}$	3
C_{X_o}	X force coefficient in steady reference condition	5
C_{X_q}	X force coefficient derivative with respect to non-dimensional pitch rate: $\frac{\partial C_X}{\partial q}\frac{2V}{\bar{c}}$	6
C_{X_α}	X force coefficient derivative with respect to angle of attack: $\frac{\partial C_X}{\partial \alpha}$	6
$C_{X_{\dot{\alpha}}}$	X force coefficient derivative with respect to non-dimensional angle of attack rate: $\frac{\partial C_X}{\partial \dot{\alpha}}\frac{2V}{\bar{c}}$	6
C_Y	Y force coefficient: $\frac{Y}{\frac{1}{2}\rho V^2 S}$	4

C_Z	Z force coefficient: $\frac{Z}{\frac{1}{2}\rho V^2 S}$	3
C_{Z_o}	Z force coefficient in steady reference condition	5
C_{Z_q}	Z force coefficient derivative with respect to non-dimensional pitch rate: $\frac{\partial C_Z}{\partial q}\frac{2V}{\bar{c}}$	5
C_{Z_α}	Z force coefficient derivative with respect to angle of attack: $\frac{\partial C_Z}{\partial \alpha}$	5
$C_{Z_{\dot{\alpha}}}$	Z force coefficient derivative with respect to non-dimensional angle of attack rate: $\frac{\partial C_Z}{\partial \dot{\alpha}}\frac{2V}{\bar{c}}$	5
$\mathbf{C_Z}$	Column vector of Z force coefficient samples	10
$\bar{c}$	Mean aerodynamic chord (reference length)	3
f	Model oscillation frequency $\sim$ Hz	9
k	Reduced frequency: $\frac{\omega \bar{c}}{2V}$	7
l_b	Aircraft model datum offset forward of balance calibration centre	15
l_c	Aircraft model datum offset forward of balance assembly centre of rotation	6
L	Rolling moment, component of fluid dynamic moment about longitudinal axis	x
M	Pitching moment, component of fluid dynamic moment about transverse axis	3
N	Yawing moment, component of fluid dynamic moment about ventral axis	x
M_t	Mach number	4
$\mathbf{P}, \mathbf{Q}, \mathbf{R}$	Intermediate matrices for pseudo-inverse computation	16
p	Roll rate, body angular velocity component about longitudinal axis	4
p_s	Ambient fluid static pressure	35
q	Pitch rate, body angular velocity component about transverse axis	3
r	Yaw rate, body angular velocity component about ventral axis	4
Re	Reynolds number: $\frac{\rho \bar{c} V}{\mu}$	7
$r_{1,\,2}$	Rotational centre registration point radii	14
S	Reference area	3
T_s	Ambient fluid absolute static temperature	35
t	Time	4

t_o	Time at steady reference condition	5
$\vec{V}$	Velocity of body with respect to fluid	3
V	Speed of body with respect to fluid	3
X	Component of fluid dynamic force along longitudinal body axis	3
$\mathbf{X}$	Array of unknown derivatives	16
Y	Component of fluid dynamic force along transverse body axis	x
Z	Component of fluid dynamic force along ventral body axis	3
x	Axis fixed in aircraft reference plane, positive forward	3
x_v	Video positioning horizontal coordinate	14
x_{v_c}	Centre of rotation in video positioning horizontal coordinates	14
y	Axis fixed normal to aircraft reference plane, positive starboard	3
y_v	Video positioning vertical coordinate	14
y_{v_c}	Centre of rotation in video positioning vertical coordinates	14
z	Axis fixed in aircraft reference plane, positive in ventral sense	3
Δ	Perturbation quantity prefix	9
Δt	Data sample time step	10
α	Angle of attack, measured from projection of velocity vector on reference plane to aircraft longitudinal axis	3
α_o	Angle of attack in steady reference condition	5
β	Angle of sideslip, measured normal from reference plane to velocity vector	3
ε	Precision test function for automated data selection	16
θ	Inclination angle, measured normal to the horizontal plane to aircraft longitudinal axis	3
θ_A	Inclination angle oscillation amplitude	9
θ_o	Inclination angle in steady reference condition	9
$\boldsymbol{\theta}$	Column vector of inclination angle perturbation samples	10
μ	Coefficient of viscosity	xi
ρ	Ambient fluid density	4
τ	Previous times	4
ω	Angular rate associated with frequency of oscillation: $2\pi f$	xi

1 Introduction

1.1 Background

The determination of an aircraft's dynamic derivatives — also referred to as damping, rotary or rotational derivatives — is an essential prerequisite for accurate modelling of linearised stability and control characteristics, as discussed in Stevens and Lewis [1], Chapter 2. Experimental investigation techniques for dynamic derivatives have evolved from those employed by Bairstow and MacLachlan [2] in the early twentieth century to the wind tunnel methods summarised by Queijo [3] and more recently to complex installations such as those of Malcolm and Schiff [4]. An extensive bibliography regarding rotary balance methods was produced by Tuttle, Kilgore and Sych [5]. Modern oscillatory balance installations include those described by Guglieri and Quagliotti [6] and by Altun and İyigün [7]. DSTO Melbourne's precursor organisations also conducted dynamic derivative investigations, such as those of Evans and Fink [8], but corporate changes have not preserved the capability. World-wide, a very few specialised installations for dynamic derivative measurement are capable of generating curving air streams, or using parabolicly-deformed models in straight air streams as discussed by Gorlin and Slezinger [9]. Otherwise, wind tunnel experimental methods are generally based on either steady rotary motion, constant-amplitude forced oscillation, or free oscillation of a model in a straight fluid stream.

Taking into account the differences in Reynolds number, Mach number, scale effects, and loads magnitude, determination of dynamic derivatives at a specified, low, reduced frequency should be possible using similar forced oscillation experimental techniques in a water tunnel. Apart from the lower costs typically associated with water tunnel work, there is the potential advantage that dynamically-scaled manoeuvres result in much lower ratios of inertial to fluid dynamic loads on the model than for the same test in a wind tunnel. Accordingly, tare loads are much lower, so loads accounting to the same level of accuracy can potentially result in lower uncertainty for the water tunnel measurements.

DSTO AVD operates an Eidetics Model 1520 water tunnel, which has been used extensively for flow visualisation tasks involving complete aircraft models. The water tunnel model support mechanism has been modified to allow independent or combined programmed rotational motions in pitch, roll and yaw, and to measure time-varying aircraft loads during motion using either two-component or five-component sting-mounted balances. Initial activities have included the study of longitudinal motion under laterally-symmetric loading conditions, using a two-component balance.

Because the water tunnel model support mechanism is restricted to rotational motion, the individual longitudinal dynamic derivatives can not be measured directly. However, combinations of measurements should allow all the individual derivatives to be determined. Under previous contracts between DSTO and Quantitative Aeronautics, techniques and software required to obtain the longitudinal aerodynamic derivatives of a representative model have been developed. Assistance has also been provided in acquisition and processing of several sets of dynamic data for the Standard Dynamics Model (SDM), an aircraft configuration developed by Beyers [10] and loosely representative of an F-16 aircraft. While these activities have been individually documented, no publicly-available summary of the work performed and the initial results obtained has yet been produced.

1.2 Purpose

This report details the underlying theory, computational implementation and experimental techniques associated with the measurement of aircraft longitudinal static and dynamic aerodynamic derivatives in the DSTO water tunnel, using a model support mechanism only capable of rotational motion.

1.3 Scope of Work

Data regarding the water tunnel balance and model support mechanism geometry, operating characteristics and force and moment data acquisition system, sufficient to adequately describe the capabilities of the installation, was collected in conjunction with DSTO staff. The information included the geometry of the strain-gauge balance and supporting structure, the operating characteristics of the system (including maximum obtainable yaw, pitch and roll rates), and the features of the data acquisition system.

Standard equations describing the unsteady aerodynamic longitudinal force and moment coefficients and small-perturbation unsteady longitudinal aerodynamic derivatives for a model undergoing simple harmonic motion in combined plunging and pitching modes were set out. The equations were used to describe the motions and fluid dynamic loadings of a model installed in the water tunnel on a sting of arbitrary length, with the dynamic balance support mechanism undergoing simple harmonic rotation in pitch. The effects of oscillation about non-zero mean angles of attack were included.

Computations were implemented in Matlab [11] or Octave [12] to extract longitudinal dynamic derivatives from time histories of SDM model position and fluid dynamic loading, oscillated under various test conditions. The functions developed were applied to sample datasets derived from tests of a SDM to validate the analytic process. Because this report is primarily focused on the underlying theory and computational implementation, it does not include a comprehensive description of tests conducted and results obtained. That information will be the subject of later reports by DSTO staff.

1.4 Symbols and Nomenclature

Throughout the following analysis, models and operating conditions are described using the nomenclature, symbols and sign conventions specified in ISO-1151 [13]. The principal relationships relevant to this report, between the wind (air-path) axis system and the body axis system, are illustrated in figure 1.

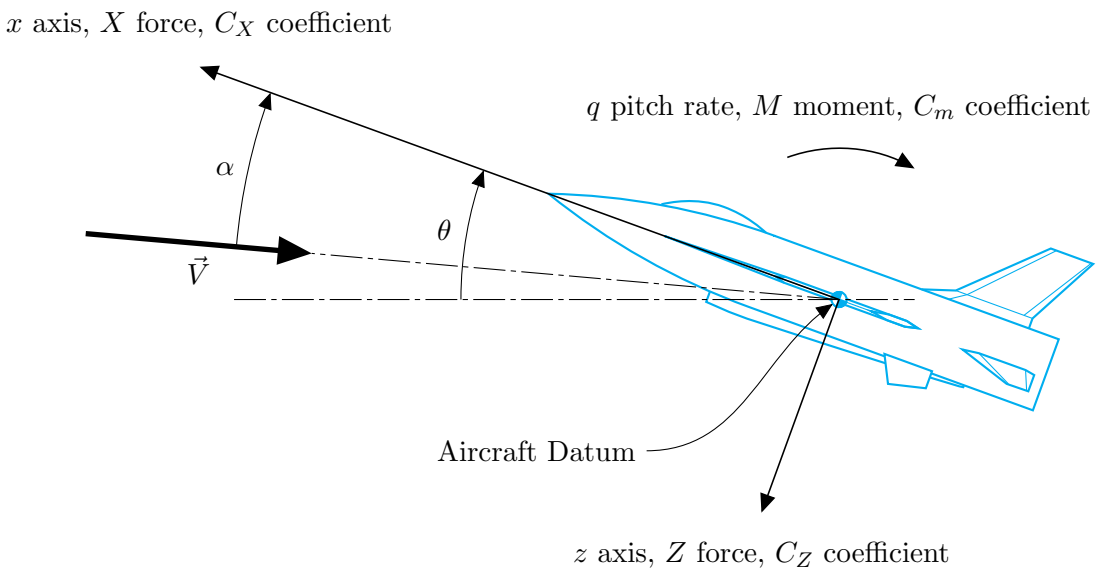

Figure 1: *Axes, orientations and symbols*

The body axes origin is considered as the datum about which aerodynamic moments are to be measured. For the SDM, the aircraft datum is fixed at 35% of the mean aerodynamic chord. All forces are positive in the corresponding positive axis direction, and all angles and moments are positive in the direction of right hand rotation about the corresponding positive axis.

2 Physical and Mathematical Basis of Test Technique

2.1 Flight Mechanics Models of Aerodynamic Loads

For an arbitrary rigid body undergoing arbitrary motion through a fluid, the pressure and shear force distributions over the body (see Anderson [14], p.16, and Etkin [15], p.158) are functions of:

1. the body shape and size, typically for aircraft described in terms of wing area (S) and a mean chord ($\bar{c}$);
2. the instantaneous orientation of the body with respect to the air-path velocity vector, specified through the angle of attack (α) and angle of sideslip (β);
3. the velocity of the body relative to the fluid, with magnitude (V);
4. the history of the body's trajectory through the fluid, to account for the upstream propagation of wake disturbance influences, for propagation delays in all directions, and for the hysteresis of flow separation processes;

5. the density of the fluid (ρ);
6. the compressibility of the fluid, typically expressed in terms of the Mach number (M_t); and
7. the Reynolds number (Re) associated with the fluid – solid interaction, indicating whether viscous or inertial effects predominate in the load distribution.

Integration of the pressure and shear force distributions yields the fluid dynamic forces and moments exerted on the body, which are conventionally expressed as non-dimensional coefficients. In three-dimensional flows, using body axes in accordance with ISO-1151 [13], the integration results in three orthogonal force coefficients (C_X, C_Y, C_Z) and three orthogonal moment coefficients (C_l, C_m, C_n). This is the minimum number of variables which can fully describe the aircraft's aerodynamic loading in arbitrary motion. For the special case of a laterally-symmetric aircraft in symmetric motion, applicable to the SDM in the water tunnel, a full description of the aerodynamic loads is provided by the three symmetric components (C_X, C_Z, C_m). These coefficients allow direct comparison of physically disparate conditions, including the application of sub-scale-model-derived coefficients directly to full-scale flight dynamic mathematical models.

Using dimensional analysis for the special case of steady flow, Anderson [14], p.30, shows that any of the aerodynamic coefficients may be expressed as a function of Mach number, Reynolds number and body orientation with respect to the flow, in a form such as

$$C_Z = \mathcal{F}(M_t, Re, \alpha, \beta) \tag{1}$$

For unsteady flow, equation 1 may be combined with Etkin's [15] expression of aerodynamic force as a functional to formally describe the aerodynamic coefficient at any time (t) as dependent on both air-path attitude history and angular rate history

$$C_Z(t) = \mathcal{F}(M_t(t), Re(t), \alpha(\tau), \beta(\tau), p(\tau), q(\tau), r(\tau)) \qquad \forall \qquad -\infty \leq \tau \leq t \tag{2}$$

which may be simplified for symmetric flight conditions by neglect of the sideslip and non-symmetric rate terms. Also, for water tunnel testing the Mach number is essentially zero and the Reynolds number variation is small, so the coefficient model need not include any dependency on these terms.

This description of the aerodynamic coefficients is consistent with the longitudinal equations of motion of a rigid aircraft, which, however expressed, require at least six scalars to completely define the aircraft state (see Stevens and Lewis [1], p.44), consisting of two translational velocity components, one angular velocity component, one attitude component and two position components. Since aerodynamic loads are essentially independent of aircraft position and attitude, and neglecting control deflections and other changes of aircraft configuration, for symmetric motion in a uniform fluid there are three aircraft system state vector components (V, α, q) which may affect the aerodynamic loading. The speed term is accounted for in the non-dimensional form. The remaining states must be included in the aerodynamic model so that it is complete to at least the same order as the equations of motion.

The formal expression in equation 2, even when simplified to symmetric loadings, is not suitable for direct inclusion in a flight dynamic model. However, using the representation

first adopted about 1911 by Bryan [16], a linearised form can be developed from Taylor series expansions of the components of equation 2 about the current time, so that

$$\alpha(\tau) = \alpha(t) + (\tau - t)\dot{\alpha}(t) + \frac{1}{2}(\tau - t)^2\ddot{\alpha}(t) + \dots \tag{3}$$

and

$$q(\tau) = q(t) + (\tau - t)\dot{q}(t) + \frac{1}{2}(\tau - t)^2\ddot{q}(t) + \dots \tag{4}$$

and therefore the aerodynamic coefficients may be written in terms of the current states and their derivatives by combining equations 3 and 4 with equation 2 as simplified for symmetric loadings without Mach or Reynolds number effects. This accounts for the aircraft trajectory short-term history effects, so that for example

$$C_Z(t) = \mathcal{F}(\alpha(t), q(t), \dot{\alpha}(t), \dot{q}(t), \ddot{\alpha}(t), \dots) \tag{5}$$

By choosing a reference condition at t_o, such that

$$\begin{aligned} C_{Z_o} &= C_Z(t_o) \quad , \\ \alpha_o &= \alpha(t_o) \quad \text{and} \\ 0 &= q(t_o) = \dot{\alpha}(t_o) = \dot{q}(t_o) = \ddot{\alpha}(t_o) = \dots \end{aligned} \tag{6}$$

and representing the aerodynamic coefficient itself by a Taylor series expansion about the reference condition in terms of the states and their derivatives,

$$C_Z(t) = C_{Z_o} + \left.\frac{\partial C_Z}{\partial \alpha}\right|_{t=t_o} (\alpha(t) - \alpha_o) + \left.\frac{\partial C_Z}{\partial q}\right|_{t=t_o} q + \left.\frac{\partial C_Z}{\partial \dot{\alpha}}\right|_{t=t_o} \dot{\alpha} + \dots \tag{7}$$

equation 7 allows a linearised description of the aerodynamic loading in terms of the aircraft's states and their derivatives. In flight mechanics usage, equation 7 is normally truncated to include only the terms shown, and the rate derivatives are non-dimensionalised using an aerodynamic time parameter $\frac{\bar{c}}{2V}$, so that

$$\begin{aligned} C_{Z_\alpha} &= \frac{\partial C_Z}{\partial \alpha} \quad , \\ C_{Z_q} &= \frac{\partial C_Z}{\partial q}\frac{2V}{\bar{c}} \quad , \\ C_{Z_{\dot{\alpha}}} &= \frac{\partial C_Z}{\partial \dot{\alpha}}\frac{2V}{\bar{c}} \quad \text{and therefore at any time} \\ C_Z &\approx C_{Z_o} + C_{Z_\alpha}(\alpha - \alpha_o) + C_{Z_q}\frac{q\bar{c}}{2V} + C_{Z_{\dot{\alpha}}}\frac{\dot{\alpha}\bar{c}}{2V} \end{aligned} \tag{8}$$

This is the conventional flight mechanics representation of an aerodynamic loading coefficient. The same form is applicable to the other longitudinal coefficients (C_X and C_m). The first coefficient derivative (C_{Z_α}) is static, because its corresponding state variable is non-zero in the reference condition described by equation 6. It, and the reference condition coefficient (C_{Z_o}), are also the only terms in the aerodynamic load representation which may be determined through static measurements in a wind or water tunnel. The remaining coefficients (C_{Z_q} and $C_{Z_{\dot{\alpha}}}$), and any higher derivatives if used, are dynamic derivatives.

The result obtained in equation 8 is limited in that it accounts for neither discontinuities, such as sharp-edged gusts, nor the long-term history of the motion (see Etkin [15], p.165 and Rodden and Giesing [17], p.272), but nevertheless is widely used in flight dynamics modelling.

Similar approximations can be derived for each of the unsteady aerodynamic force and moment coefficients. Where the assumption of a symmetric flight condition is not valid, cross-derivatives extend equation 8 to account for the effects of sideslip, roll rate, and yaw rate. In the worst case, for all six aerodynamic load coefficients on an asymmetric aircraft in an asymmetric flight condition, there may be at least 72 derivatives to be determined. Methods for estimating most of the derivatives are set out in DATCOM [18]; alternatively they may be derived from computational aerodynamics, wind tunnel test or flight test.

Fortunately, many of these derivatives make negligible contributions to the total force coefficients. Zipfel [19], pp.226-235; Stevens and Lewis [1], pp.66-67, pp.107-109; Etkin [15], pp.159-160; and Roskam [20], ch.4 each set out their own rules for neglecting various derivatives, depending on the flight vehicle configuration. For longitudinal derivatives expressed in body axes, typically only C_{Z_α}, C_{X_α}, C_{m_α}, C_{m_q} and $C_{m_{\dot{\alpha}}}$ are considered of primary importance. The normal force dynamic terms C_{Z_q} and $C_{Z_{\dot{\alpha}}}$ are generally of secondary importance. The longitudinal force dynamic terms C_{X_q} and $C_{X_{\dot{\alpha}}}$ are generally ignored.

All of the important longitudinal dynamic derivatives can be measured separately by using a model and balance installation capable of oscillating in both pitch and plunge, although the quality of measurements vary widely. Typically a pitching motion about the aircraft datum is used to measure the dynamic derivatives as a combined term (such as $C_{Z_q} + C_{Z_{\dot{\alpha}}}$), while a plunging motion allows measurement of the angle of attack rate term (such as $C_{Z_{\dot{\alpha}}}$) in isolation. A recent description of the use of a wind tunnel model in the measurement of dynamic derivatives, including a valuable discussion of sources of inaccuracy and means of dealing with it, is provided by Kim, Murphy and Klein [21], in one of a series of papers relating to NASA dynamic derivative testing. Although not an exact analogue of water tunnel testing, many of the problems are similar and may be dealt with similarly. The advantage of the technique discussed in the current report over an installation using separate pitching and plunging oscillations is that the separate longitudinal derivatives can be measured using a model and balance installation capable of rotational oscillation only.

2.2 Water Tunnel Installation and Operating Conditions

The geometry of the balance assembly installed in the DSTO Eidetics Model 1520 water tunnel is shown in figure 2, including a variable length (l_c) model sting arrangement. For the purpose of longitudinal derivative measurement, the balance support assembly moves only in rotation, mechanised through a belt-driven C-strut.

Note: Dimensions in mm

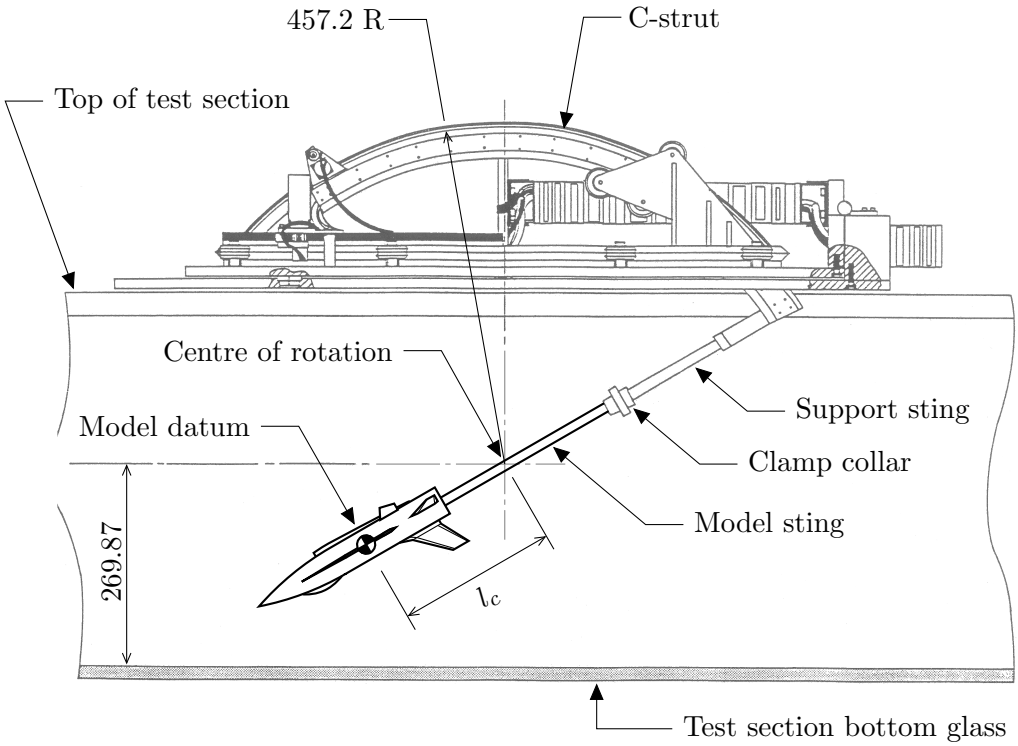

Figure 2: *DSTO Water tunnel balance geometry*

Arbitrary model motion is programmable, but longitudinal derivative measurement requires only steady, uniform, sinusoidal oscillation in pitch about an arbitrary mean inclination angle. The nominal operating conditions and limits of the balance and water tunnel are shown in table 1.

Table 1: *DSTO water tunnel and balance operating conditions*

Parameter	Minimum	Normal	Maximum
Angles (deg):			
Roll	-360	0	+360
Pitch	0	—	65
Yaw	-20	0	+20
Angular Rates (deg.s^{-1}):			
Roll	0	—	12
Pitch	0	—	6
Yaw	0	—	8
Flow speed (m.s^{-1})	0	0.1	0.6
Reynolds number (Re) [1]	0	8.59 $\times 10^3$	5.15 $\times 10^4$
Reduced Frequency (k) [2]	0	0.091	0.015

1. Based on reference length of 86.2 mm at 20 °C.
2. Based on reference length of 86.2 mm at maximum pitch rate.

The SDM model as constructed for use in the DSTO water tunnel has a mean aerodynamic chord of 86.2 mm, which is also used as the reference length in table 1 for computation of test Reynolds numbers and reduced frequencies. This length is also representative of most models for which the water tunnel might be suitable. The Reynolds numbers achievable in the water tunnel compare unfavourably with operating conditions for the types of aircraft represented by the SDM. As discussed in section 2.1, the aerodynamic load coefficients to be measured are functions of Re. Typically Reynolds number sensitivity in such coefficients is most obvious for values below about half a million. Accordingly, the difference between tunnel test and flight Reynolds number is large enough to potentially affect the validity of measured dynamic derivatives, depending on the geometry of the aircraft under test. The discrepancy is unavoidable for a small tunnel using water at ambient conditions as the working fluid, but should be specifically considered when planning a dynamic derivative test program.

The achievable reduced frequencies, however, are more than adequate for dynamic derivative testing. The available pitch rates, even at the maximum tunnel velocity, will allow a series of tests reasonably spaced in reduced frequency, from which the zero-frequency derivatives may be extrapolated. For example, a tunnel speed of about 0.1 $m.s^{-1}$ is typically used for flow visualisation. At this speed, using a moderate-amplitude oscillation, a reduced frequency in the order of 0.01, which may adequately approximate the zero-frequency case without extrapolation, is achieved with a maximum pitch rate of 0.012 $deg.s^{-1}$. The low rates required have the additional advantage of minimising inertial load variation and sting deflection due to inertial loading during the oscillation, thereby reducing the effect of one source of measurement imprecision.

The magnitudes of the forces involved in testing at this scale and Reynolds number may be quite low. For the SDM model in the DSTO water tunnel, tested at the normal operating speed of 0.1 $m.s^{-1}$, and operating over an oscillatory pitch attitude range of 0.5 degrees, the amplitude of the corresponding lift force oscillatory component is in the order of 0.04 N. This rises to about 1.2 N at the maximum operating speed. The moments generated are proportionately small. Such loads require the balance sensor and analog-to-digital converter systems to be optimised for the intended load range, and may cause problems with bridge stability and drift. If absolutely necessary, the required load range can be minimised by re-zeroing about the mean angle of attack for each test point, so that the entire sensor range corresponds to the unsteady load component. However, this is undesirable from both test efficiency and measurement quality aspects. Whatever approach is adopted, rigorous control of accuracy, precision and test technique is essential in this application.

2.3 Model Installation Kinematics

The kinematics of a model installed on a variable length sting and oscillating sinusoidally in pitch around a rotation centre not necessarily coincident with the model datum are illustrated in figure 3.

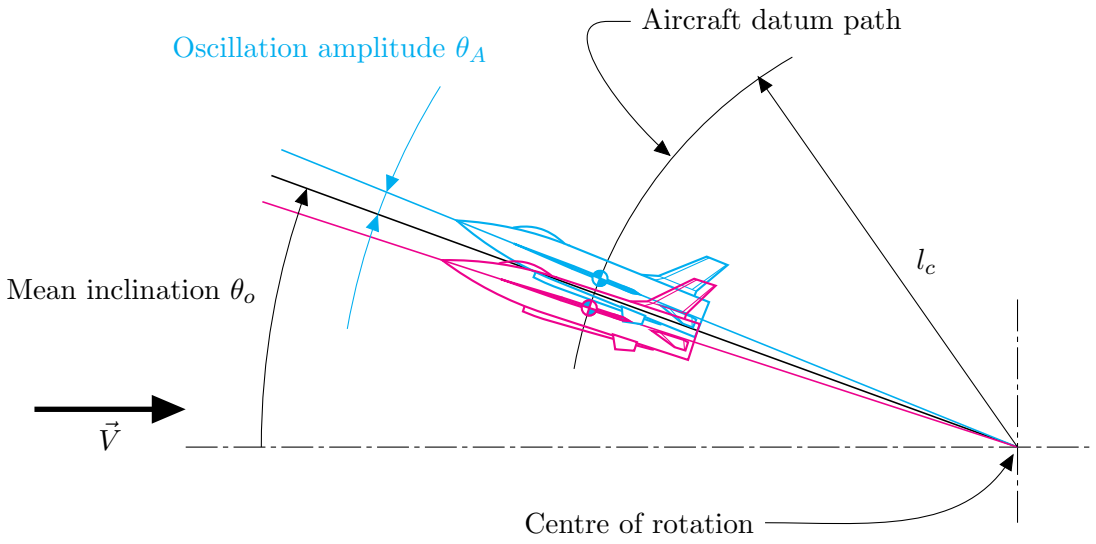

Figure 3: *Pitching model kinematic relationships*

The DSTO water tunnel installation's kinematics are adequately described by this representation. The model oscillates about a mean inclination angle θ_o, at constant frequency f in a steady stream of velocity V, so that

$$\begin{aligned} \omega &= 2\pi f \qquad \text{and} \\ k &= \frac{\omega \bar{c}}{2V} \end{aligned} \tag{9}$$

Observing the geometry of the installation, and assuming small oscillations about a non-zero mean angle (θ_o), the time-varying relationships between angles and rates, expressed in terms of perturbations and total quantities, are:

1. Inclination angle perturbation:

$$\Delta\theta = \theta_A \sin \omega t \tag{10}$$

2. Inclination angle:

$$\begin{aligned} \theta &= \theta_o + \Delta\theta \\ &= \theta_o + \theta_A \sin \omega t \end{aligned} \tag{11}$$

3. Pitch rate:

$$\begin{aligned} q &= \dot{\theta} \\ &= \dot{\Delta\theta} \\ &= \theta_A \omega \cos \omega t \end{aligned} \tag{12}$$

4. Angle of attack:

$$\alpha = \theta - \frac{l_c}{V}\dot{\theta} \tag{13}$$

where l_c is the distance by which the centre of rotation lies aft of the aircraft datum along the x body axis. This approximation applies for low to moderate angles of attack, and for normal velocities due to pitch rate which are small in comparison with the free stream velocity.

5. Angle of attack rate:

$$\begin{aligned} \dot{\alpha} &= \dot{\theta} - \frac{l_c}{V}\ddot{\theta} \\ &= \dot{\theta} + \frac{l_c}{V}\theta_A\omega^2 \sin\omega t \\ &= \dot{\theta} + \frac{l_c}{V}\omega^2\Delta\theta \end{aligned} \tag{14}$$

By combining these relationships with the linearised aerodynamic model of equation 8, any of the total aerodynamic load coefficients can be expressed entirely in terms of the inclination angle and its first derivative.

2.4 Data Analysis and Processing

Using the pitching moment coefficient as an example (the technique may be applied identically to all aerodynamic coefficients), the linearised equation for an aerodynamic coefficient may be written in the same form as equation 8, so that

$$C_m = C_{m_0} + C_{m_\alpha}\Delta\alpha + C_{m_q}\frac{q\bar{c}}{2V} + C_{m_{\dot{\alpha}}}\frac{\dot{\alpha}\bar{c}}{2V} \tag{15}$$

In the particular case of sinusoidal rotational oscillation about a mean angle, by employing the kinematic relationships between the various angles and angular rates in accordance with equations 10 through 14, the moment coefficient may be equivalently expressed in terms of the perturbation pitch angle only as

$$C_m = C_{m_0} + C_{m_\alpha}\left(\Delta\theta - \frac{l_c}{V}\dot{\theta}\right) + \left(C_{m_q} + C_{m_{\dot{\alpha}}}\right)\frac{\bar{c}}{2V}\dot{\theta} + C_{m_{\dot{\alpha}}}\frac{\bar{c}}{2V}\frac{l_c}{V}\omega^2\Delta\theta \tag{16}$$

This equation is true at any sample time during the oscillatory motion.

The data recorded during a water tunnel test include time-correlated sequences of inclination angle, normal force and pitching moment. After translation of the loads to the model datum, and normalisation to coefficient form, the data may be represented as column vectors

$$\begin{aligned} \boldsymbol{\theta} &= \begin{bmatrix}\Delta\theta(t_o) & \Delta\theta(t_o+\Delta t) & \Delta\theta(t_o+2\Delta t) & \ldots\end{bmatrix}^T & , \\ \mathbf{C_Z} &= \begin{bmatrix}C_Z(t_o) & C_Z(t_o+\Delta t) & C_Z(t_o+2\Delta t) & \ldots\end{bmatrix}^T & \text{and} \\ \mathbf{C_m} &= \begin{bmatrix}C_m(t_o) & C_m(t_o+\Delta t) & C_m(t_o+2\Delta t) & \ldots\end{bmatrix}^T \end{aligned} \tag{17}$$

As the model oscillation is sinusoidal at constant frequency, equations 10 and 12 in combination will determine an inclination angular rate vector $\dot{\boldsymbol{\theta}}$ from the analytic or numerical derivative of the inclination angle perturbation vector. Equation 16 therefore forms the basis of a matrix equation where each row of the matrices contains the data sampled at one time during the motion. It takes the form

$$\begin{aligned}\mathbf{C_m} &= \begin{bmatrix}\mathbf{1} & \left(\boldsymbol{\theta} - \frac{l_c}{V}\dot{\boldsymbol{\theta}}\right) & \frac{\bar{c}}{2V}\dot{\boldsymbol{\theta}} & \frac{\bar{c}}{2V}\frac{l_c}{V}\omega^2\boldsymbol{\theta}\end{bmatrix}\begin{bmatrix}C_{m_0}\\ C_{m_\alpha}\\ \left(C_{m_q}+C_{m_{\dot{\alpha}}}\right)\\ C_{m_{\dot{\alpha}}}\end{bmatrix}\\ &= \mathbf{A}\begin{bmatrix}C_{m_0}\\ C_{m_\alpha}\\ \left(C_{m_q}+C_{m_{\dot{\alpha}}}\right)\\ C_{m_{\dot{\alpha}}}\end{bmatrix}\end{aligned} \tag{18}$$

where $\mathbf{1}$ is a column vector of ones. Although equation 17 represents the samples of angular position and fluid dynamic load as being in monotonic temporal sequence, this is not essential for equation 18 to remain valid, provided the sample time for each row of all column vectors is consistent. Because the water tunnel model's frequency of oscillation is constant and known, this equation is linear. If a significant number of samples is taken, equation 18 represents an over-determined system of linear equations which can be solved in a minimum norm sense using singular value decomposition or pseudo-inverse techniques to determine estimates of both the aerodynamic coefficients which form the right-hand matrix and the uncertainty associated with the estimation process.

However, as it stands the angular position and velocity sample matrix ($\mathbf{A}$) of equation 18 is rank deficient, since column 2 is a linear combination of columns 3 and 4. To avoid this problem, two special cases must be considered.

2.4.1 Centre of Rotation Coincident with Aircraft Datum

If the centre of rotation is coincident, to engineering precision, with the aircraft datum (i.e. $l_c = 0$ in figure 3), equation 18 simplifies to

$$\begin{aligned}\mathbf{C_m} &= \begin{bmatrix}\mathbf{1} & \boldsymbol{\theta} & \frac{\bar{c}}{2V}\dot{\boldsymbol{\theta}}\end{bmatrix}\begin{bmatrix}C_{m_0}\\ C_{m_\alpha}\\ \left(C_{m_q}+C_{m_{\dot{\alpha}}}\right)\end{bmatrix}\\ &= \mathbf{A_R}\begin{bmatrix}C_{m_0}\\ C_{m_\alpha}\\ \left(C_{m_q}+C_{m_{\dot{\alpha}}}\right)\end{bmatrix}\end{aligned} \tag{19}$$

The $\mathbf{A_R}$ matrix in equation 19 is not rank deficient, and may be solved in a least squares or minimum-norm sense to provide the best available estimates of the reference condition pitching moment coefficient (C_{m_0}), the static derivative pitching moment coefficient (C_{m_α}) and the combined dynamic derivative pitching moment coefficients ($C_{m_q} + C_{m_{\dot{\alpha}}}$). An identical computation, replacing $\mathbf{C_m}$ by the z-wise force coefficient vector $\mathbf{C_Z}$, will produce the force coefficient static and combined dynamic derivatives.

2.4.2 Pre-Determined Static or Combined Dynamic Derivatives

If the centre of rotation is displaced from the aircraft datum (i.e. $l_c \neq 0$ in figure 3), equation 18 can be rearranged to avoid rank deficiency provided either of the static aerodynamic derivative or combined dynamic derivative coefficients is known in advance. For the DSTO water tunnel, this information can be obtained by performing a curve fit of data obtained under the same test conditions but with the centre of rotation coincident with the aircraft datum, in accordance with equation 19. Equation 18 may then be rearranged in any of the following alternative forms, with a different reduced angular velocity and position sample matrix in each case.

1. When C_{m_α} only is known:

$$\begin{aligned}\left[\mathbf{C_m} - C_{m_\alpha}\left(\boldsymbol{\theta} - \frac{l_c}{V}\dot{\boldsymbol{\theta}}\right)\right] &= \begin{bmatrix}\mathbf{1} & \frac{\bar{c}}{2V}\dot{\boldsymbol{\theta}} & \frac{\bar{c}}{2V}\frac{l_c}{V}\omega^2\boldsymbol{\theta}\end{bmatrix}\begin{bmatrix}C_{m_0}\\ (C_{m_q}+C_{m_{\dot\alpha}})\\ C_{m_{\dot\alpha}}\end{bmatrix}\\ &= \mathbf{A_R}\begin{bmatrix}C_{m_0}\\ (C_{m_q}+C_{m_{\dot\alpha}})\\ C_{m_{\dot\alpha}}\end{bmatrix}\end{aligned} \tag{20}$$

2. When $\left(C_{m_q} + C_{m_{\dot\alpha}}\right)$ only is known:

$$\begin{aligned}\left[\mathbf{C_m} - \left(C_{m_q}+C_{m_{\dot\alpha}}\right)\frac{\bar{c}}{2V}\dot{\boldsymbol{\theta}}\right] &= \begin{bmatrix}\mathbf{1} & \left(\boldsymbol{\theta} - \frac{l_c}{V}\dot{\boldsymbol{\theta}}\right) & \frac{\bar{c}}{2V}\frac{l_c}{V}\omega^2\boldsymbol{\theta}\end{bmatrix}\begin{bmatrix}C_{m_0}\\ C_{m_\alpha}\\ C_{m_{\dot\alpha}}\end{bmatrix}\\ &= \mathbf{A_R}\begin{bmatrix}C_{m_0}\\ C_{m_\alpha}\\ C_{m_{\dot\alpha}}\end{bmatrix}\end{aligned} \tag{21}$$

3. When both C_{m_α} and $\left(C_{m_q} + C_{m_{\dot\alpha}}\right)$ are known:

$$\begin{aligned}\left[\mathbf{C_m} - C_{m_\alpha}\left(\boldsymbol{\theta} - \frac{l_c}{V}\dot{\boldsymbol{\theta}}\right) - \left(C_{m_q}+C_{m_{\dot\alpha}}\right)\frac{\bar{c}}{2V}\dot{\boldsymbol{\theta}}\right] &= \begin{bmatrix}\mathbf{1} & \frac{\bar{c}}{2V}\frac{l_c}{V}\omega^2\boldsymbol{\theta}\end{bmatrix}\begin{bmatrix}C_{m_0}\\ C_{m_{\dot\alpha}}\end{bmatrix}\\ &= \mathbf{A_R}\begin{bmatrix}C_{m_0}\\ C_{m_{\dot\alpha}}\end{bmatrix}\end{aligned} \tag{22}$$

In each case, the left hand side forms a single column vector and the $\mathbf{A_R}$ matrix is full-rank. Any of these equations may be solved in a least squares or minimum-norm sense for the separate dynamic derivative aerodynamic coefficient $C_{m_{\dot\alpha}}$. The precise technique used will be constrained by method availability within a particular computational package, and by computational performance and stability, as discussed in section 3.4.

Since both static and combined dynamic derivatives are obtainable from equation 19, use of equation 22 is preferable because it explicitly enforces the constraint that the separated dynamic derivatives C_{m_q} and $C_{m_{\dot\alpha}}$ as determined during testing with the centre

of rotation and aircraft datum non-coincident should sum to exactly equal the combined derivative $C_{m_q} + C_{m_{\dot{\alpha}}}$ as determined with the centre of rotation and aircraft datum coincident. An identical process, replacing $\mathbf{C_m}$ by $\mathbf{C_Z}$, is used for determination of the force coefficient separated dynamic derivatives.

3 Implementation of Technique

3.1 Overview

A Matlab- or Octave-based computational framework was developed for data from the DSTO water tunnel, based on the models described in sections 2.3 and 2.4. All code was designed and tested to function identically in either computational environment with appropriate toolboxes installed. The code:

1. reads time histories of model attitude and body axes forces and moments, from datasets supplied in the form of Excel spreadsheets;
2. combines model attitude and tunnel velocity data to determine angle of attack;
3. converts body axes forces and moments to non-dimensional coefficients, using fluid properties as defined by IAPWS-95 [22] and IAPS-85 [23];
4. fits a sinusoid to time history of inclination angle, using an iterative method based on IEEE Standard 1057 [24], in order to determine the forcing frequency, amplitude and phase; and
5. determines the longitudinal static and dynamic derivatives for pitching moment and normal force based on the curve fitting process outlined in section 2.4.

The functional elements, additional to normal Matlab toolbox components, are detailed in Appendix A. Soft copies of these functions accompany this report.

3.2 Geometric Relationships

The relationships developed in equations 17 through 22 depend heavily on the physical geometry of the installation, as well as on its kinematics. In particular, the relative positions of the centre of rotation, the model datum and the balance calibration centre must be known accurately in order to obtain satisfactory results. The models used in the DSTO water tunnel are small, with the SDM's 86.2 mm mean aerodynamic chord being typical, and a model's longitudinal datum is often close to its neutral point. Therefore, an error of the order of 1 mm in relative position of the three relevant centres can result in static margin errors in the order of 50 percent, and may even result in sign changes for pitching moment derivatives. Further uncertainty in these geometric relationships may be introduced by sting and balance stiffness effects. Because results are so significantly affected by inaccuracy in these measurements, extreme care in experimental technique is required to ensure that they are measured accurately and maintained during tests.

To minimise geometric problems, a technique was developed for optical determination of any centre of rotation offset from the model datum (l_c), using a video system to obtain Cartesian coordinates of two registration points on the model during an oscillation cycle. The relationship of video-derived coordinates (x_v, y_v) to the body axes system (x, z) is arbitrary, dependent on the video system processing technique. It is also irrelevant, because the video coordinates' only purpose is to determine the position of the centre of rotation relative to the registration points. Since the position of the model datum relative to the registration points may be determined by physical measurement, the radii of the registration points relative to the centre of rotation are sufficient to fully establish the relationship between the model datum and the centre of rotation. Geometry for the installation without an extended sting is shown in figure 4.

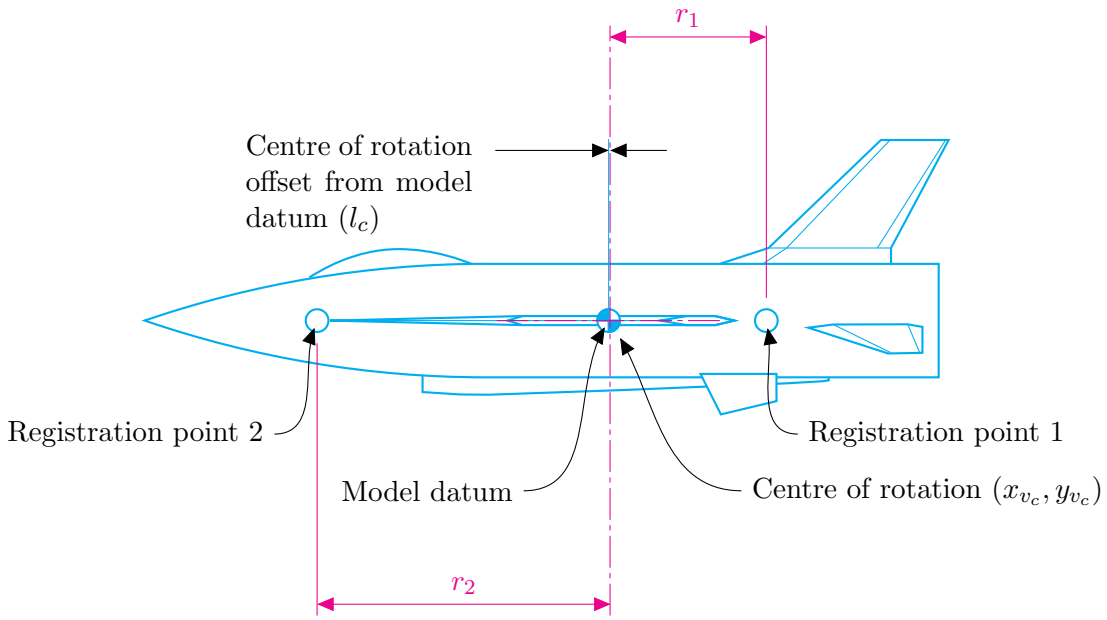

Figure 4: *Reference point geometric relationships*

The geometric relationships based on these coordinates were solved in the function **fit-circle**, iteratively fitting two circular arcs to the registration point paths for a minimum-norm estimate of the relative position of the centre of rotation. Output from the function for the SDM installation is shown in figure 5. Comparison of the fitted registration point radii for the SDM with physical measurement of the distance between the two registration points (199.84 mm) indicates that the centre of rotation, the model datum and the registration points are not exactly collinear. The SDM centre of rotation is offset 5.8 mm z-wise and 0.28 mm x-wise from the model datum. Although the z-wise offset has little effect on the dynamic derivative measurements, it should be avoided in future model installations. Neglecting the z-wise offset, $l_c = -0.28$ mm for the SDM installation without extended sting. That is, the centre of rotation is 0.28 mm forward of the aircraft datum. For a typical water tunnel test point using a working section velocity of 0.1 m.s^{-1}, the aerodynamic time factor in equation 18 becomes $l_c/V = 0.0028$, which should allow the approximation in equation 19 to be employed.

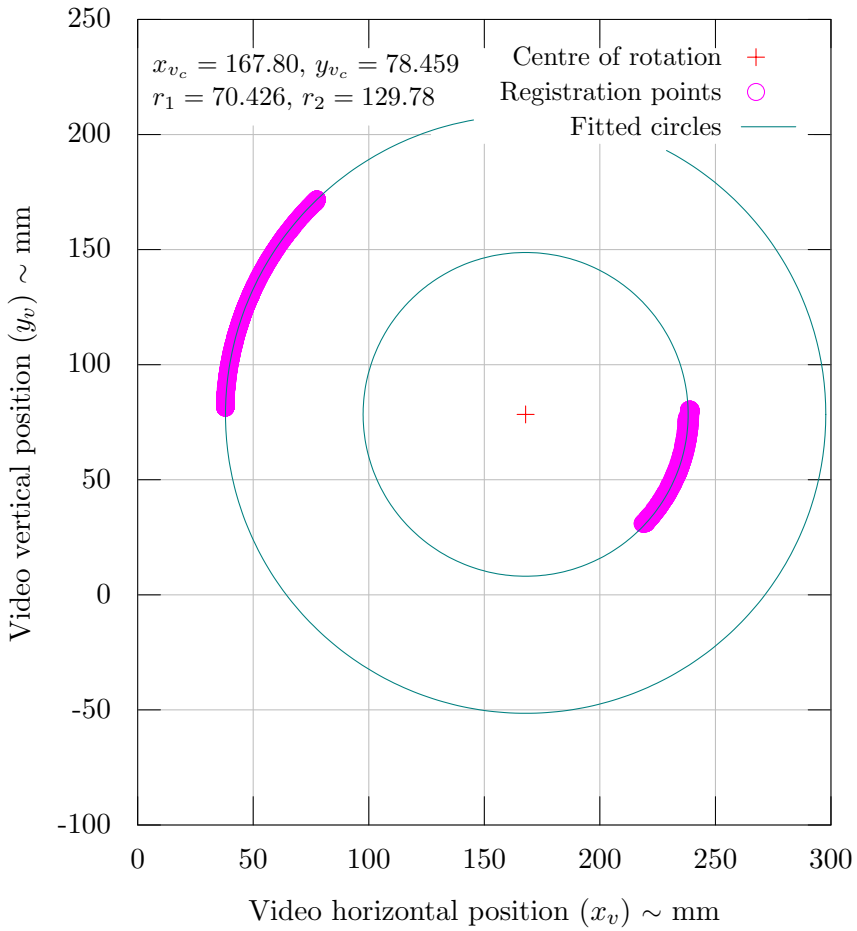

Figure 5: *Rotational geometry determination*

The location of the balance calibration centre with respect to the model datum only requires static measurement, since it depends only on the interface between model and balance. For the SDM installation, the balance centre has been measured to be $l_b = -0.59$ mm, placing the balance centre slightly forward of the model datum. The measured moment coefficients may then be transferred to the aircraft model datum using the relationship

$$C_m = C_{m_{\text{balance}}} + \frac{l_b}{\bar{c}} C_{Z_{\text{balance}}} \tag{23}$$

before further processing for the dynamic derivatives.

3.3 Automated Data Selection

A principal assumption underlying equations 18 through 22 is that both the input model inclination angle and the resultant force and moment coefficients follow a steady, constant-amplitude, constant-frequency sinusoid. For this assumption to be reasonably satisfied in the water tunnel, starting transients must be allowed to dissipate before a data set is selected for curve fitting. An automated data selection process has been included in

functions **fitCombinedDeriv** and **fitSeparatedDeriv**, in order to satisfy the steady oscillation constraint without requiring user intervention.

The data selection process is commenced with the full sequential arrays of angular position ($\boldsymbol{\theta}$), angular velocity ($\dot{\boldsymbol{\theta}}$), and either force coefficient ($\mathbf{C_Z}$) or moment coefficient ($\mathbf{C_m}$) data available. The arrays are to be reduced in length by eliminating the earliest samples until a coefficient convergence criterion is satisfied. Taking the computation of combined moment coefficient dynamic derivatives as an example, for the ith selection step the procedure is:

1. An estimate of the mean coefficient and its derivatives is obtained using the basic pseudo-inverse method (signified in equation 24 by $^+$) described in section 3.4, so that
$$\begin{bmatrix} C_{m_0} \\ C_{m_\alpha} \\ (C_{m_q} + C_{m_{\dot\alpha}}) \end{bmatrix}_i = \mathbf{A_R}_i^+ \ \mathbf{C_m}_i \tag{24}$$

2. A precision test function is established based on the difference between the current estimated values and those obtained using the previous data sequence, so that,
$$\varepsilon_i = \begin{bmatrix} 1 & 1 & 1 \end{bmatrix} \left| \begin{bmatrix} C_{m_0} \\ C_{m_\alpha} \\ (C_{m_q} + C_{m_{\dot\alpha}}) \end{bmatrix}_i - \begin{bmatrix} C_{m_0} \\ C_{m_\alpha} \\ (C_{m_q} + C_{m_{\dot\alpha}}) \end{bmatrix}_{i-1} \right| \tag{25}$$

3. If the test function ε_i is greater than 0.01, one complete oscillation is removed from the beginning of the $\boldsymbol{\theta}$ array, and the corresponding data samples are removed from the angular velocity and load coefficient arrays. Equation 24 is then re-formed using the reduced arrays and the process is repeated. The data sequence arrays are not reduced by more than half their length, since that would imply an entirely unstable test condition.

The comparatively simple convergence test condition is justified because the coefficients on which it operates are already normalised, and have only a small range of typical values. However, it has not been tested using a wide range of models and tunnel operating conditions, and cannot be considered an optimum data selection test. In future, different tests are likely to require different data selection techniques.

3.4 Pseudo-Inverse Computation

The computations implemented in functions **fitCombinedDeriv** and **fitSeparatedDeriv** to solve equations 19 through 22 are performed by the Matlab or Octave backslash operator. In accordance with the Matlab manual [11], this operator minimises the largest singular value of $(\mathbf{A_R} * \mathbf{X} - \mathbf{C_m})$, where $\mathbf{X}$ represents the array of unknown derivatives forming the right hand matrix in equations 19 through 22, using Householder reflections to compute an orthogonal-triangular factorisation such that

$$\mathbf{A_R P} = \mathbf{QR} \tag{26}$$

where $\mathbf{P}$ is a permutation, $\mathbf{Q}$ is orthogonal and $\mathbf{R}$ is upper triangular. The least squares solution is computed with

$$\mathbf{X} = \mathbf{P}\left(\mathbf{R} \setminus \left(\mathbf{Q}^T \mathbf{C_m}\right)\right) \tag{27}$$

using LAPACK [25] routines. Octave performs an equivalent solution. However, these details are transparent to the user. The choice of the backslash operator for the computational implementation was principally for programmatic convenience. Various other methods of solution for over-determined systems of equations could equally be applied to equations 19 through 22.

The performance of the technique was tested by generating simulated test data based on known values for the coefficients and derivatives, then analysing them in accordance with sections 2.4 and 3. An example set of simulated test data is listed in table 2.

Table 2: *Simulated data - pitching moment test*

Parameter	Value	Units
$\bar{c}$	86.2	mm
l_c	150	mm
k	0.01	
V	0.1	$\mathrm{m.s}^{-1}$
θ_o	10.0	deg
θ_A	0.25	deg
C_{m_0}	0.02	
C_{m_α}	0.2	
C_{m_q}	-6.0	
$C_{m_{\dot{\alpha}}}$	-2.0	

In addition to the basic data derived from table 2 incorporated in equation 16, two cases with Gaussian noise added to each of the simulated pitching moment coefficient measurements were tested. In the test context, “noise” refers to any component of the measured signal at a frequency other than that of the model oscillation, whether that component originated from the physics of the flow, from mechanical or other excitation, or from the data acquisition process. Signal-to-noise ratios (SNRs) of 60 dB, an extremely noisy signal, and 100 dB, a relatively clean signal, were chosen as representative of a wide range of experimental results. With and without the extended sting, the worst-case, 60 dB noise-augmented, data provided moment coefficient responses which were fitted as shown in figure 6. An identical process was followed for the 100 dB data.

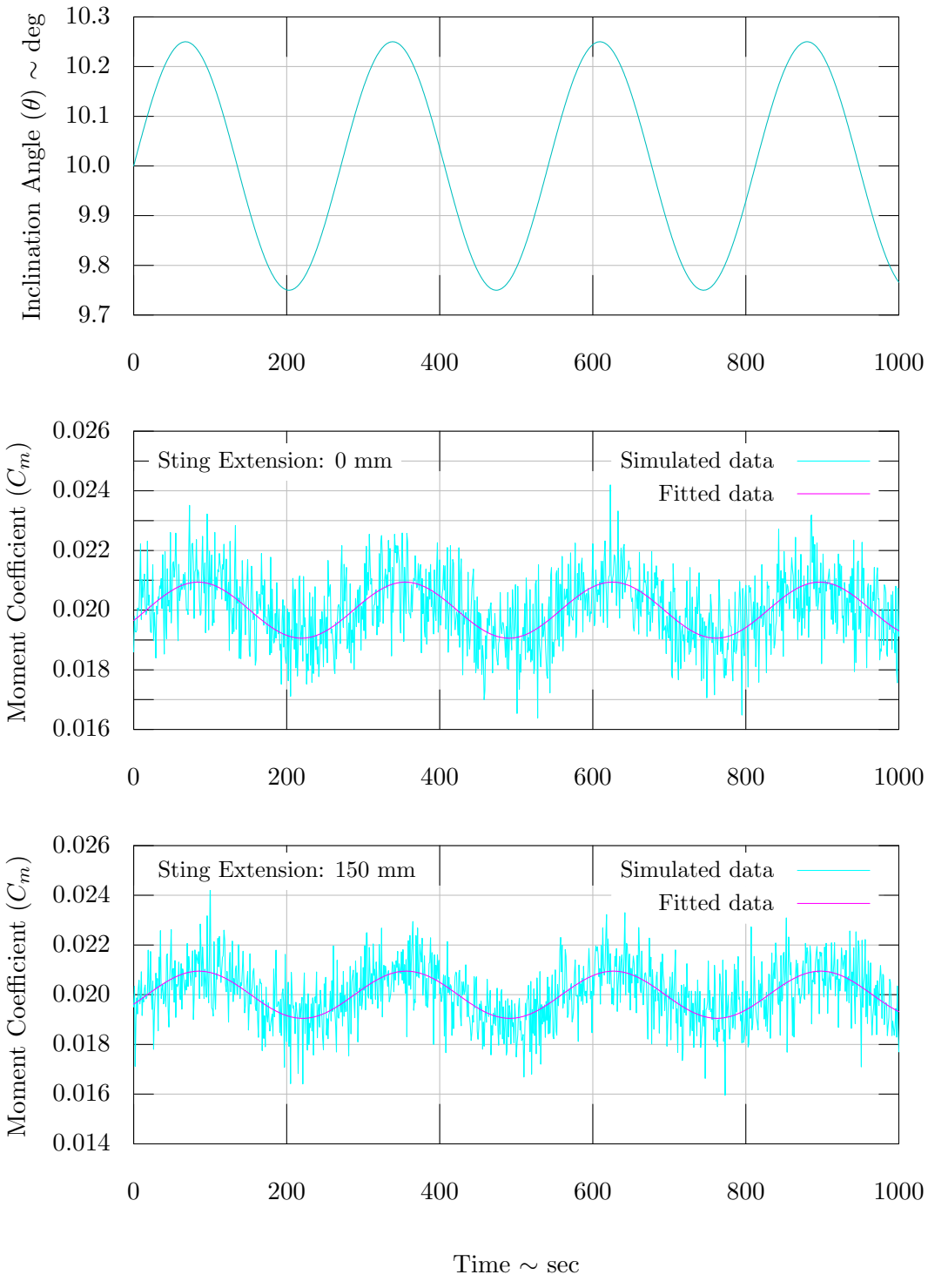

Figure 6: *Simulated data - pitching moment - 60 dB SNR noise added*

Recovered derivatives from the curve fitting process, with and without noise, are listed in table 3, with the original derivatives included for comparison. For these tests, equation 22 was used for determining the separated dynamic derivatives.

Table 3: *Recovered data - pitching moment test*

Parameter	Simulation Input	Recovered Derivatives		
		No Noise	60 dB SNR	100 dB SNR
C_{m_α}	0.200	0.200	0.198	0.200
$C_{m_q} + C_{m_{\dot\alpha}}$	-8.00	-8.00	-7.906	-8.01
C_{m_q}	-6.00	-6.00	-12.22	-6.51
$C_{m_{\dot\alpha}}$	-2.00	-2.00	4.315	-1.50

With a noise-free signal, exact recovery of all the derivatives was achieved. With both noisy signals, excellent recovery of the static and combined dynamic derivatives was achieved, but the result for the separate aerodynamic angle rate derivative ($C_{m_{\dot\alpha}}$), and therefore of the pitch damping (C_{m_q}) which depended on it, was of unacceptable quality in the 60 dB case. However, the results for the low-noise cases are consistent with the ranges of accuracy suggested by Roskam [20] table 4.13, and indicate that the basic method is sound, provided the experimental technique can achieve signal-to-noise ratios in the order of 100 dB or better.

3.5 Program Usage

The computational framework envisages that initial measurements will be taken with the water tunnel model's datum essentially coincident with the balance mechanism centre of rotation, using the standard length (i.e. 0 mm sting extension) sting. These measurements allow the static derivatives and combined dynamic derivatives to be determined at a particular reduced frequency and Reynolds number, over a sequence of angles of attack. These measurements alone are sufficient to determine the static and combined dynamic measurements, using function **fitAllCombinedDeriv**. A second set of measurements, using an extended sting, should repeat the previous tests under the same conditions. Static, combined dynamic, and separated dynamic derivatives can then be computed using both sets of measurements as inputs to function **fitAllSeparatedDeriv**.

The parameters and returns for both functions are shown in Appendix A. All datasets must be installed on disks accessible from the Matlab or Octave workspace. For use with models other than the SDM, the functions must be edited to change:

1. the model reference area;
2. the model reference length; and
3. the model datum, balance centre and centre of rotation relationships.

For the separated derivative computation, the sting extension length must also be supplied when **fitAllSeparatedDeriv** is called. All other required data is automatically extracted from the spreadsheets containing the recorded data. An Octave workspace during a typical data processing session is shown in figure 7. The data used was derived from preliminary

tests, and the results shown indicate the method, not the measured characteristics of the SDM.

```
x = fitAllSeparatedDeriv( 'S00/*.XLS', 'S30/*.XLS', 300, 'true' )
Dynamic Separated Derivative Water Tunnel SDM Data Processing

    Reference area ~ mm^2          : 17404
    Reference length ~ mm          : 86.2
    Without sting extension :
     Balance centre distance aft of datum ~ mm  : -0.59
     Rotation centre distance aft of datum ~ mm : -0.28
    Sting extension length ~ mm    : 300
    Ambient atmospheric pressure ~ hPa         : 1013.2
    Processing file "01 dynamic S00 2010 02 04.XLS" ...
    Processing file "01 dynamic S30 2010 02 04.XLS" ...
x = {
  ssFile = 01 dynamic S00 2010 02 04.XLS
  xsFile = 01 dynamic S30 2010 02 04.XLS
  alpha = -1.1580e-05
  k =  0.099535
  Rn =  9858.8
  xsAlpha = -1.1255e-05
  xsK =  0.099607
  xsRn =  9851.6
  Cz = -0.014738
  Cm =  0.0019623
  Cza = -3.8691
  Cma =  0.15048
  Czq = -28.383
  Cmq = -2.7980
  Czad =  25.423
  Cmad = -2.5801
  Czqad = -2.9604
  Cmqad = -5.3781
  sigmaz = 4.4117e-04   8.2182e-02   2.0799e+00   2.2745e+00   9.2074e-01
  sigmam = 8.5674e-05   1.2863e-02   3.9205e-01   4.1575e-01   1.3838e-01
  nz =  847
  nm =  1356
  xnz =  1186
  xnm =  847
  xsLsting =  0.15000
  thetaA =  0.0087090
  xsThetaA =  0.0087089
}
```

Figure 7: *Workspace interaction example*

Descriptions of the input parameters and the results returned are provided in Appendix A. All curve fitting results may be plotted and saved for later review if required. The programs as written are almost trivial to use, but a lack of user understanding of the rather complex underlying processes is likely to lead to unreliable results.

4 Conclusions and Recommendations

It is theoretically possible to resolve the individual components of the main longitudinal dynamic derivatives using a water tunnel balance undergoing purely rotary oscillations, by combining results measured with different balance sting lengths. Experiments with simulated inputs have confirmed the general validity of the technique, and provided some indication of the data quality from which acceptable results might be obtained.

The difference between tunnel test and flight Reynolds number is large enough to potentially affect the validity of measured dynamic derivatives, depending on the geometry of the aircraft under test. The discrepancy should be specifically considered when planning a dynamic derivative test program. Because of the small scales, low dynamic pressures and consequent low loads to be recorded by a water tunnel balance system, and the considerable involvement of differencing in the computational treatment of the experimental results, results of acceptable quality require rigorous control of accuracy and precision at every stage of the experimental and computational process. Measurement and quality control of balance and model geometry are particularly important.

Static and combined dynamic derivatives can be reliably and accurately computed in the presence of very high noise levels on the measured signals, but separated dynamic derivatives require signal-to-noise ratios in the order of 100 dB or better for adequate performance.

The dynamic derivative computation process functions acceptably without requiring user interaction, but this does not eliminate the need for user understanding of the process and detailed review of the results obtained.

References

1. Stevens, B. L., and Lewis, F. L., *Aircraft Control and Simulation*, John Wiley and Sons Inc., 1992.

2. Bairstow, L., and MacLachlan, L. A., *The Experimental Determination of Rotary Coefficients*, R and M 78, ARC, March 1913.

3. Queijo, M. J., 'Methods of Obtaining Stability Derivatives', in *Performance and Dynamics of Aerospace Vehicles*, NASA SP-258, NASA, Washington, D.C., 1971, pp 71-102.

4. Malcolm, G. N., and Schiff, L. B., *Recent Development in Rotary-Balance Testing of Fighter Aircraft Configurations at NASA Ames Research Center*, NASA TM-86714, NASA, Washington, D.C., July 1985.

5. Tuttle, M. H., Kilgore, R. A., and Sych, K. L., *Rotary Balances – A Selected, Annotated Bibliography*, NASA TM-4105, NASA, Washington, D.C., March 1989.

6. Guglieri, G., and Quagliotti, F. B., *Dynamic Stability Derivatives Evaluation in a Low-Speed Wind Tunnel*, J. Aircraft, Vol. 30, N^o 3, 0021-8669, 1993, pp 421-423.

7. Altun, M., and İyigün, I., *Dynamic Stability Derivatives of a Maneuvering Combat Aircraft Model*, J. Aeronautics and Space Technologies, Vol. 1, N^o 3, January 2004, pp 19-27.

8. Evans, J. M., and Fink, P. T., *Determination of l_p by Free Oscillations*, Report A.39, CSIR Division of Aeronautics, Fishermen's Bend, Melbourne, October 1945.

9. Gorlin, S. M., and Slezinger, I. I., *Wind Tunnels and Their Instrumentation (Aeromekhanicheskie izmerenia. Metody i pribory)*, trans. P. Boltiansky, Israel Program for Scientific Translations, Jerusalem, published as NASA TT-F-346, NASA, Washington, D.C., 1966.

10. Beyers, M. E., *SDM Pitch- and Yaw-Axis Stability Derivatives*, Paper 85-1827, AIAA, August 1985.

11. Anon., *Documentation for MathWorks Products, R2010a*, viewed 26 August 2010 at http://www.mathworks.com/access/helpdesk/help/helpdesk.html.

12. Eaton, J. W., Bateman, D., and Hauberg, S., *GNU Octave Manual Version 3*, Network Theory Ltd, UK, August 2008.

13. Anon., *Flight Dynamics – Concepts, Quantities and Symbols*, Parts 1-9, ISO 1151, International Organization for Standardization, Switzerland, 1982-1998.

14. Anderson, J. D., *Fundamentals of Aerodynamics*, Second edition, McGraw-Hill International Editions, New York, 1991.

15. Etkin, B., *Dynamics of Atmospheric Flight*, John Wiley and Sons, New York, 1972.

16. Bryan, G. H., *Stability in Aviation: An Introduction to Dynamical Stability as applied to the Motions of Aeroplanes*, Macmillan and Co., Limted, London, 1911.

17. Rodden, W. P., and Giesing, J. P., *Application of Oscillatory Aerodynamic Theory to Estimation of Dynamic Stability Derivatives*, J. Aircraft, Vol. 7, N^o 3, May-June 1970, pp 272-275.

18. Hoak, D. E., et al., *USAF Stability and Control DATCOM*, Flight Control Division, Air Force Flight Dynamics Laboratory, Wright-Patterson Air Force Base, Ohio, September 1970.

19. Zipfel, P. H., *Modeling and Simulation of Aerospace Vehicle Dynamics*, AIAA Education Series, Reston, VA, 2000.

20. Roskam, J., *Airplane Flight Dynamics and Automatic Flight Controls*, Roskam Aviation and Engineering Corporation, Ottawa, KS, 1979.

21. Kim, S., Murphy, P. C., and Klein, V., *Evaluation and Analysis of F-16XL Wind Tunnel Data From Dynamic Tests*, AIAA-2003-5396, AIAA Atmospheric Flight Mechanics Conference and Exhibit, Austin, Texas, August 2003.

22. Anon., *Release on the IAPWS Formulation 1995 for the Thermodynamic Properties of Ordinary Water Substance for General and Scientific Use*, IAPWS-95, International Association for the Properties of Water and Steam, Fredericia, Denmark, September 1996.

23. Anon., *Revised Release on the IAPS Formulation 1985 for the Viscosity of Ordinary Water Substance*, IAPS-85, International Association for the Properties of Water and Steam, Vejle, Denmark, August 2003.

24. Anon., *IEEE Standard for Digitizing Waveform Recorders*, IEEE Standard 1057, TC-10 of IEEE Instrumentation and Measurement Society, 1994.

25. Anderson, E., Bai, Z., Bischof, C., Blackford, S., Demmel, J., Dongarra, J., Du Croz, J., Greenbaum, A., Hammarling, S., McKenney, A., and Sorensen, D., *LAPACK Users' Guide*, 3rd Ed., Society for Industrial and Applied Mathematics, 22 August 1999.

Appendix A Matlab/Octave Function Reference

Functions

- [x] = concatenateCombinedDeriv (x1, x2, ..., xn)
- [x] = concatenateSeparateDeriv (x1, x2, ..., xn)
- [y1, ..., yn] = allNoZeros (x1, ..., xn)
- [x] = fitAllCombinedDeriv (filePattern, plotfit)
- [x] = fitAllSeparatedDeriv (ssFilePattern, xsFilePattern, lsting, plotfit)
- [xc, yc, r1, r2] = fitcircle (x, y, r1w, r2w)
- [k, theta0, Cf0, Cfa, Cfqad, sigma, thetadot, iter, thetaA] = fitCombinedDeriv (theta, time, Cf, tstar, lcstar)
- [k, theta0, Cf0, Cfad, Cfq, sigma, thetadot, iter, thetaA] = fitSeparatedDeriv (theta, time, Cf, tstar, lcstar, Cfa, Cfqad)
- [a0, a1, f, theta] = fitSine (y, t, selData, hfig)
- [phi0, phiR, phiR_d, phiR_d2] = HelmholtzFunction (delta, tau)
- [t, theta, Fz, My, V, Ta] = loadDataFile (fileName)
- [y, iy] = noZeros (x)
- plotCombinedDeriv (x, nSd)
- plotSeparateDeriv (x, nSd)
- [rho] = waterDensity (Pa, Ta)
- [Pa] = waterPressure (rho, Ta)
- [mu] = waterViscosity (rho, Ta)

A.1 Description

All the m-files included with this report are usable in either Matlab or Octave workspaces, with identical calling syntax. They require that basic toolboxes are installed in either environment. Because the DSTO water tunnel data are produced in Excel spreadsheet format, these functions interrogate the spreadsheets directly. The interrogation techniques used require that a spreadsheet API, one of Excel, Java/Apache POI or Java/JExcelAPI must be installed on the computer in use. The m-files make some assumptions about the relationships between directory structures, spreadsheet file names and file content. The assumptions are detailed in individual function descriptions. It is the user's responsibility to ensure that these assumptions are satisfied. In general, the user should only require to interact with the high level functions x and y. The other functions are used internally during the computations.

A.2 Function Documentation

A.2.1 [x] = concatenateCombinedDeriv(*x1*, *x2*, ..., *xn*)

The function **concatenateCombinedDeriv** combines dynamic derivative results from two or more test runs which are in the format generated by the function **fitAllCombinedDeriv**. As many inputs as desired may be included. The conditions for each test point of subsequent inputs must match the α, k, and Re values of the first input.

Parameters

x1*, *x2*, ..., *xn are structures containing the fields specified as outputs from function **fitAllCombinedDeriv**.

Returns

x is the concatenated structure in the same format as any of the individual inputs.

A.2.2 [x] = concatenateSeparateDeriv(*x1*, *x2*, ..., *xn*)

The function **concatenateSeparateDeriv** combines dynamic derivative results from two or more test runs which are in the format generated by the function **fitAllSeparatedDeriv**. As many inputs as desired may be included. The conditions for each test point of subsequent inputs must match the α, k, and Re values of the first input.

Parameters

x1*, *x2*, ..., *xn are structures containing the fields specified as outputs from function **fitAllSeparatedDeriv**.

Returns

x is the concatenated structure in the same format as any of the individual inputs.

A.2.3 [y1, ..., yn] = allNoZeros (*x1*, ..., *xn*)

The function **allNoZeros** removes possible leading and trailing zeros from parallel data streams, reducing them all to the minimum length which can remove the zeros from all streams. It also removes NaNs, which may be generated by Excel from invalid cell references.

Parameters

x1*, ..., *xn are parallel arrays, each of m samples containing a time sequence of data, possibly with leading and trailing zeros or NaNs or extreme values.

Returns

y1, ..., yn are parallel arrays, each of $\leq m$ samples from the corresponding original sequences ***x1*, ..., *xn*** of data with leading and trailing zeros and NaNs truncated.

A.2.4 [x] = fitAllCombinedDeriv (*filePattern*, *plotfit*)

The function **fitAllCombinedDeriv** uses a series of datasets containing attitude, force and moment data from a rotary balance sinusoidal oscillation to determine a sequence of static (e.g. C_{m_α}) and combined dynamic (e.g. $\left(C_{m_q} + C_{m_{\dot{\alpha}}}\right)$) derivatives of force and moment coefficients with respect to attitude and attitude rates. It has been written specifically for the SDM, but requires only changes to the reference data to be used with other models.

Parameters

filePattern is the fully-qualified path to all the files to be processed, including wildcards as necessary. These may be Excel spreadsheets in the format required by loadDataFile, or Matlab/Octave data files containing data equivalent to the output from loadDataFile.

plotfit is an optional Boolean parameter, 'true' or 'false', which specifies whether plots of the curve fits are to be saved in the input file directory. Its default value is 'false'.

Returns

x is a structure containing the following fields, where n is the number of input files which satisfied the requested file pattern, so that each input file provided the data for one pair of static and combined dynamic derivatives:

file is an array of the n names of the Excel (.xls) or Matlab/Octave (.mat) files which were sources for the processed results.

alpha is an array of the approximate mean angle of attack in degrees for each of the n test points.

k is an array of the reduced frequencies for each of the n test points.

Rn is an array of the Reynolds numbers for each of the n test points.

Cz is an array of the mean normal force coefficients, C_{Z_o}, for each of the n test points.

Cm is an array of the mean pitching moment coefficients, C_{m_o}, for each of the n test points.

Cza is an array of the normal force coefficient derivatives with respect to angle of attack C_{Z_α}, per radian, for each of the n test points.

Cma is an array of the pitching moment coefficient derivatives with respect to angle of attack C_{m_α}, per radian, for each of the n test points.

Czqad is an array of the sum of derivatives $\left(C_{Z_q} + C_{Z_{\dot{\alpha}}}\right)$, per radian, for each of the n test points.

Cmqad is an array of the sum of derivatives $\left(C_{m_q} + C_{m_{\dot{\alpha}}}\right)$, per radian, for each of the n test points.

sigmaz is a two-dimensional $n \times 3$ array of the estimated standard deviations of the fitted parameters C_{Z_o}, C_{Z_α}, and $\left(C_{Z_q} + C_{Z_{\dot{\alpha}}}\right)$ in that sequence, for each of the n test points. These represent uncertainty due to curve fitting, not the overall uncertainty of the dynamic derivative measurement process.

sigmam is a two-dimensional $n \times 3$ array of the estimated standard deviations of the fitted parameters C_{m_o}, C_{m_α}, and $\left(C_{m_q} + C_{m_{\dot{\alpha}}}\right)$ in that sequence, for each of the n test points. These represent uncertainty due to curve fitting, not the overall uncertainty of the dynamic derivative measurement process.

nz is an array of the number of force coefficient derivative fits performed for each of the n test points.

nm is an array of the number of moment coefficient derivative fits performed for each of the n test points.

thetaA is the oscillation amplitude, in radians, for each of the n test points.

A.2.5 [x] = fitAllSeparatedDeriv (*ssFilePattern*, *xsFilePattern*, *lsting*, *plotfit*)

The function **fitAllSeparatedDeriv** uses a series of datasets containing attitude, force and moment data from a rotary balance sinusoidal oscillation, with and without a sting extension, to determine a sequence of static (e.g. C_{m_α}) and separated dynamic (e.g. C_{m_q}, $C_{m_{\dot{\alpha}}}$) derivatives of force and moment coefficients with respect to attitude and attitude rates. The files with and without sting extension must have been recorded at the same reduced frequencies and mean inclination angles, and at similar Reynolds numbers. They must be named in the same angle of attack sequence. The input files may be Excel spreadsheets in the format required by loadDataFile, or Matlab/Octave data files containing data equivalent to the output from loadDataFile. The function has been written specifically for the SDM, but requires only changes to the reference data to be used with other models.

Parameters

ssFilePattern is the fully-qualified path to files to be processed, from tests not using an extended sting, including wildcards as necessary.

xsFilePattern is the fully-qualified path to files to be processed, from tests using the extended sting, including wildcards as necessary.

lsting is the sting extension length, expressed in mm.

plotfit is an optional Boolean parameter, 'true' or 'false', which specifies whether plots of the curve fits are to be saved in the input file directory. Its default value is 'false'.

Returns

x is a structure containing the following fields, where n is the number of pairs of input files which satisfied the requested file patterns, so that each pair of input files provided the data for one static and two separate dynamic derivatives:

ssFile is an array of the n names of the Excel (.xls) or Matlab/Octave (.mat) files acquired without the sting extension which were sources for the processed results.

xsFile is an array of the n names of the Excel (.xls) or Matlab/Octave (.mat) files acquired with the sting extension which were sources for the processed results.

alpha is an array of the approximate mean angle of attack in degrees for each of the n test points.

k is an array of the reduced frequencies for each of the n test points.

Rn is an array of the Reynolds numbers for each of the n test points.

Cz is an array of the mean normal force coefficients, C_{Z_o}, for each of the n test points.

Cm is an array of the mean pitching moment coefficients, C_{m_o}, for each of the n test points.

Cza is an array of the normal force coefficient derivatives with respect to angle of attack C_{Z_α}, per radian, for each of the n test points.

Cma is an array of the pitching moment coefficient derivatives with respect to angle of attack C_{m_α}, per radian, for each of the n test points.

Czq is an array of the normal force coefficient derivatives with respect to normalised pitch rate C_{Z_q}, per radian, for each of the n test points.

Czad is an array of the normal force coefficient derivatives with respect to normalised aerodynamic angle rate $C_{Z_{\dot\alpha}}$, per radian, for each of the n test points.

Czqad is an array of the sum of derivatives $\left(C_{Z_q} + C_{Z_{\dot\alpha}}\right)$, per radian, for each of the n test points.

Cmq is an array of the pitching moment coefficient derivatives with respect to normalised pitch rate C_{m_q}, per radian, for each of the n test points.

Cmad is an array of the pitching moment coefficient derivatives with respect to normalised aerodynamic angle rate $C_{m_{\dot\alpha}}$, per radian, for each of the n test points.

Cmqad is an array of the sum of derivatives $\left(C_{m_q} + C_{m_{\dot\alpha}}\right)$, per radian, for each of the n test points.

sigmaz is a two-dimensional $n \times 5$ array of the estimated standard deviations of the fitted parameters C_{Z_o}, C_{Z_α}, C_{Z_q}, $C_{Z_{\dot\alpha}}$ and $\left(C_{Z_q} + C_{Z_{\dot\alpha}}\right)$ in that sequence, for each of the n test points. These represent uncertainty due to curve fitting, not the overall uncertainty of the dynamic derivative measurement process.

sigmam is a two-dimensional $n \times 5$ array of the estimated standard deviations of the fitted parameters C_{m_o}, C_{m_α}, C_{m_q}, $C_{m_{\dot\alpha}}$ and $\left(C_{m_q} + C_{m_{\dot\alpha}}\right)$ in that sequence, for each of the n test points. These represent uncertainty due to curve fitting, not the overall uncertainty of the dynamic derivative measurement process.

nz is an array of the number of force coefficient derivative fits performed for each of the n test points.

nm is the number of moment coefficient derivative fits performed for each of the n test points.

thetaA is the oscillation amplitude, in radians, for each of the n test points.

A.2.6 [xc, yc, r1, r2] = fitcircle (*x*, *y*, *r1w*, *r2w*)

The function **fitcircle** finds the centre of the circle which is a minimum-norm fit to a set of n Cartesian data coordinates, nominally on the circumference of a circle or on the circumferences of two concentric circles.

Parameters

x is an array of x-wise locations of circumferential points.

y is an array of y-wise locations of circumferential points which correspond with the points in ***x***.

r1w is an index vector which corresponds with the points in ***x*** and ***y***. An element equals 1 if the point is on radius 1 and 0 otherwise. This vector is not required if all input points fall on a single circle.

r2w is an index vector which corresponds with the points in ***x*** and ***y***. An element equals 1 if the point is on radius 2 and 0 otherwise. This vector is not required if all input points fall on a single circle.

Returns

xc is the x-wise location of the fitted circle's centre.

yc is the y-wise location of the fitted circle's centre.

r1 is the radius of fitted circle 1.

r2 is the radius of fitted circle 2. This value will not be returned if all input points fall on a single circle.

A.2.7 [k, theta0, Cf0, Cfa, Cfqad, sigma, thetadot, iter, thetaA] = fitCombinedDeriv (*theta*, *time*, *Cf*, *tstar*, *lcstar*)

The function **fitCombinedDeriv** uses attitude and force or moment coefficient data from a rotary balance sinusoidal oscillation to determine the static and combined dynamic derivatives of the force or moment coefficient with respect to the kinematic variables.

Parameters

theta is an array of n sequential samples, representing the inclination angle of the SDM at each time when balance data samples were acquired, in degrees above horizontal.

time is an array of n sequential samples, representing the times at which water tunnel balance data samples were acquired, in seconds.

Cf is an array of n sequential samples, representing a fluid dynamic load coefficient, such as C_{Z_o} or C_{m_o}, for the SDM at each time when balance data samples were acquired.

tstar is an aerodynamic time parameter, the ratio of the model reference length to the flow velocity ($\bar{c}/2V$), in seconds.

lcstar is an aerodynamic time parameter, the velocity-normalised distance of the rotation centre aft of the aircraft model datum (l_c/V), in seconds.

Returns

k is the reduced frequency for this test point as determined from the inclination angle history.

theta0 is the mean inclination angle about which the pitch oscillation takes place, in radians.

Cf0 is the mean ***Cf*** coefficient, such as C_{Z_o} or C_{m_o}.

Cfa is the static derivative, determined dynamically, of the ***Cf*** coefficient with respect to angle of attack, such as C_{Z_α} or C_{m_α}, per radian.

Cfqad is the sum of the ***Cf*** coefficient dynamic derivatives, such as $\left(C_{Z_q} + C_{Z_{\dot{\alpha}}}\right)$ or $\left(C_{m_q} + C_{m_{\dot{\alpha}}}\right)$, per radian.

sigma is an array of the estimated standard deviations of the fitted parameters such as C_{Z_o}, C_{Z_α}, and $\left(C_{Z_q} + C_{Z_{\dot{\alpha}}}\right)$, in that sequence. These represent uncertainty due to curve fitting, not the overall uncertainty of the dynamic derivative measurement process.

thetadot is an array of n sequential samples, representing the rate of change of model inclination angle at each time when balance data samples were acquired, in rad.s^{-1}.

iter is the number of coefficient curve fits performed for this test point.

thetaA is the oscillation amplitude, in radians.

A.2.8 [k, theta0, Cf0, Cfad, Cfq, sigma, thetadot, iter, thetaA] = fitSeparatedDeriv (*theta*, *time*, *Cf*, *tstar*, *lcstar*, *Cfa*, *Cfqad*)

The function **fitSeparatedDeriv** uses attitude and force or moment coefficient data from a rotary balance sinusoidal oscillation with an extended sting, plus combined derivative data from a rotary balance sinusoidal oscillation without the extended sting, to determine the static and separated dynamic derivatives of the force or moment coefficient with respect to the kinematic variables.

Parameters

theta is an array of n sequential samples, representing the inclination angle of the SDM at each time when balance data samples were acquired, in degrees above horizontal.

time is an array of n sequential samples, representing the times at which water tunnel balance data samples were acquired, in seconds.

Cf is an array of n sequential samples, representing a fluid dynamic load coefficient, such as C_{Z_o} or C_{m_o}, for the SDM at each time when balance data samples were acquired.

tstar is an aerodynamic time parameter, the ratio of the model reference length to the flow velocity ($\bar{c}/2V$), in seconds.

lcstar is an aerodynamic time parameter, the velocity-normalised distance of the rotation centre aft of the aircraft model datum (l_c/V), in seconds.

Cfa is the static derivative, determined dynamically, of the ***Cf*** coefficient with respect to angle of attack, such as C_{Z_α} or C_{m_α}, as determined by a zero-length sting test under the same test conditions, per radian.

Cfqad is the sum of the ***Cf*** coefficient dynamic derivatives, such as $\left(C_{Z_q} + C_{Z_{\dot{\alpha}}}\right)$ or $\left(C_{m_q} + C_{m_{\dot{\alpha}}}\right)$, as determined by a zero-length sting test under the same test conditions, per radian.

Returns

k is the reduced frequency for this test point as determined from the inclination angle history.

theta0 is the mean inclination angle about which the pitch oscillation takes place, in radians.

Cf0 is the mean ***Cf*** coefficient, such as C_{Z_o} or C_{m_o}.

Cfad is the dynamic derivative of the ***Cf*** coefficient with respect to non-dimensionalised angle of attack rate, such as $C_{Z_{\dot{\alpha}}}$ or $C_{m_{\dot{\alpha}}}$, per radian.

Cfq is the dynamic derivative of the ***Cf*** coefficient with respect to non-dimensionalised pitch rate, such as C_{Z_q} or C_{m_q}, per radian.

sigma is an array of the estimated standard deviations of the fitted parameters such as C_{Z_o}, $C_{Z_{\dot{\alpha}}}$, and C_{Z_q}, in that sequence. These represent uncertainty due to curve fitting, not the overall uncertainty of the dynamic derivative measurement process.

thetadot is an array of n sequential samples, representing the rate of change of model inclination angle at each time when extended-sting balance data samples were acquired, in rad.s^{-1}.

iter is the number of coefficient curve fits performed for this test point.

thetaA is the oscillation amplitude for the extended-sting test point, in radians.

A.2.9 [a0, a1, f, theta] = fitSine (*y*, *t*, *selData*, *hfig*)

The function **fitSine** fits a sine wave of the form

$$y = a_0 + a_1 \sin(2\pi f t + \theta)$$

to the data supplied. It is based on the IEEE Standard 1057 algorithm for 4-parameter sine fitting. There is an option for interactive graphical selection of a subset of the supplied data for curve fitting. There is also an option to plot the result and the original data for comparison. The convergence criterion is angular velocity converged to within 10^{-6}.

Parameters

y is an array of n sequential data samples, with even temporal spacing.

t is either an array of n evenly-spaced sequential sample times, or a single constant sample time-step. Consistent units, normally seconds, are required.

selData is a Boolean parameter, 'true' or 'false', which specifies whether to interactively select a subset of the input data for curve fitting.

hfig is an optional figure handle, only to be supplied if a plot of the fitted data result is required.

Returns

a0 is a constant offset of the fitted sinusoid.

a1 is the amplitude of the fitted sinusoid.

f is the frequency of the fitted sinusoid, having units compatible with the input time base. For ***t*** in seconds, **f** is returned in Hz.

theta is the phase lead of the fitted curve relative to the input time base. It is returned in radians.

A.2.10 [phi0, phiR, phiR_d, phiR_d2] = HelmholtzFunction (*delta*, *tau*)

The function **HelmholtzFunction** computes the ideal gas and residual parts of the dimensionless Helmholtz free energy in terms of the non-dimensional temperature and density, based on IAPWS-95, "Release on the IAPWS Formulation 1995 for the Thermodynamic Properties of Ordinary Water Substance for General and Scientific Use".

Parameters

delta is the ambient water density ratio ($\rho/322$ for density in kg.m^{-3}).

tau is the inverse temperature ratio ($647.096/T_s$ for temperature in K).

Returns

phi0 is the dimensionless Helmholtz free energy ideal gas component.

phiR is the dimensionless Helmholtz free energy residual component.

phiR_d is the partial derivative of the residual component with respect to the density ratio.

phiR_d2 is the second partial derivative of the residual component with respect to the density ratio.

A.2.11 [t, theta, Fz, My, V, Ta] = loadDataFile (*filename*)

The function **loadDataFile** uses Matlab or Octave versions of function **xlsread** to access information about a spreadsheet containing DSTO water tunnel Standard Dynamics Model test data, and to return the load versus displacement time histories contained therein to the calling program. It requires that a spreadsheet API, one of Excel, Java/Apache POI or Java/JExcelAPI, be installed on the computer in use.

Parameters

filename is the fully qualified name of a spreadsheet file from which data in DSTO water tunnel output format is to be read. The data is assumed to be in a worksheet named "SDM Dynamic Data", in columns having headers which include the words "Time", "Angle", "Force", and "Pitching". Headers for "Velocity" and "Temperature" are optional, but if they are not found the required values will be requested interactively.

Returns

t is an array of n sequential samples, representing the times at which water tunnel balance data samples were acquired, in seconds.

theta is an array of n sequential samples, representing the pitch attitude of the SDM at each time when balance data samples were acquired, in degrees above horizontal.

Fz is an array of n sequential samples, representing the z-wise fluid dynamic load on the SDM at each time when balance data samples were acquired, in N.

My is an array of n sequential samples, representing the pitching moment due to fluid dynamic load on the SDM at each time when balance data samples were acquired, in N.m.

V is the water tunnel working section velocity, in m.s^{-1}.

Ta is the water tunnel ambient temperature, in deg C.

A.2.12 [y, iy] = noZeros (*x*)

The function **noZeros** removes possible leading and trailing zeros from data streams. It also removes NaNs, which may be generated by Excel from invalid cell references.

Parameters

x is an array of n samples containing a time sequence of data, possibly with leading and trailing zeros or NaNs or extreme values.

Returns

y is an array of $\leq n$ samples from the original sequence ***x*** of data with leading and trailing zeros and NaNs truncated.

iy is an index vector of the positions of the returned sequence **y** within the original sequence ***x***.

A.2.13 plotCombinedDeriv(*x*, *nSd*)

The function **plotCombinedDeriv** plots dynamic derivative results from the format generated by the function **fitAllCombinedDeriv**.

Parameters

x is a structure containing the fields specified as outputs from function **fitAllCombinedDeriv**.

nSd is an optional parameter which specifies the number of standard deviations to be used for plot error bars. The default value is 1.

A.2.14 plotSeparateDeriv(*x*, *nSd*)

The function **plotSeparateDeriv** plots dynamic derivative results from the format generated by the function **fitAllSeparatedDeriv**.

Parameters

x is a structure containing the fields specified as outputs from function **fitAllSeparatedDeriv**.

nSd is an optional parameter which specifies the number of standard deviations to be used for plot error bars. The default value is 1.

A.2.15 [rho] = waterDensity (*Pa*, *Ta*)

The function **waterDensity** computes the density of water, using the dimensionless Helmholtz function, in terms of the non-dimensional temperature and pressure, based on IAPWS-95, "Release on the IAPWS Formulation 1995 for the Thermodynamic Properties of Ordinary Water Substance for General and Scientific Use". This is an inverse iterative solution. It tests stable on the data in this report, but if instability occurs when applied to other data the damping parameter may need adjustment.

Parameters

Pa is the ambient water static pressure p_s, in Pa.

Ta is the ambient water static temperature T_s, in K.

Returns

rho is the ambient water density ρ, in kg.m^{-3}.

A.2.16 [Pa] = waterPressure (*rho*, *Ta*)

The function **waterPressure** computes the pressure in water, using the dimensionless Helmholtz function, in terms of the non-dimensional temperature and density, based on IAPWS-95, "Release on the IAPWS Formulation 1995 for the Thermodynamic Properties of Ordinary Water Substance for General and Scientific Use".

Parameters

rho is the ambient water density ρ, in kg.m^{-3}.

Ta is the ambient water static temperature T_s, in K.

Returns

Pa is the ambient water static pressure p_s, in Pa.

A.2.17 [mu] = waterViscosity (*rho*, *Ta*)

The function **waterViscosity** computes the viscosity of water, based on "Revised Release on the IAPWS Formulation 1985 for the Viscosity of Ordinary Water Substance", August 2003.

Parameters

rho is the ambient water density ρ, in kg.m^{-3}.

Ta is the ambient water static temperature T_s, in K.

Returns

mu is the ambient water viscosity μ, in Pa.s.

DEFENCE SCIENCE AND TECHNOLOGY ORGANISATION DOCUMENT CONTROL DATA	1. CAVEAT/PRIVACY MARKING

2. TITLE	3. SECURITY CLASSIFICATION
A Technique for Measurement of Static and Dynamic Longitudinal Aerodynamic Derivatives Using the DSTO Water Tunnel	Document (U) Title (U) Abstract (U)
4. AUTHOR	5. CORPORATE AUTHOR
Daniel M. Newman	Defence Science and Technology Organisation 506 Lorimer St, Fishermans Bend, Victoria 3207, Australia

6a. DSTO NUMBER	6b. AR NUMBER	6c. TYPE OF REPORT	7. DOCUMENT DATE
DSTO–TR–2599	AR-015-087	Technical Report	December, 2011

8. FILE NUMBER	9. TASK NUMBER	10. SPONSOR	11. No. OF PAGES	12. No. OF REFS
2010/1125948/1	DST 07/250	DSTO	36	25

13. URL OF ELECTRONIC VERSION	14. RELEASE AUTHORITY
http://dspace.dsto.defence.gov.au/dspace/	Chief, Air Vehicles Division

15. SECONDARY RELEASE STATEMENT OF THIS DOCUMENT

Approved for Public Release

OVERSEAS ENQUIRIES OUTSIDE STATED LIMITATIONS SHOULD BE REFERRED THROUGH DOCUMENT EXCHANGE, PO BOX 1500, EDINBURGH, SOUTH AUSTRALIA 5111

16. DELIBERATE ANNOUNCEMENT

No Limitations

17. CITATION IN OTHER DOCUMENTS

No Limitations

18. DSTO RESEARCH LIBRARY THESAURUS

Water tunnels
Flow visualization
Aerodynamics
Aircraft models
Fluid dynamics

19. ABSTRACT

The DSTO water tunnel's balance and rotary support mechanism provides a measurement capability for longitudinal dynamic derivatives. This report documents the underlying theory and computational implementation of a technique which uses the water tunnel for determination of normal force and pitching moment coefficient derivatives with respect to angle of attack, non-dimensional pitch rate and angle of attack rate.